Available online at www.sciencedirect.com
SCIENCE DIRECT®
Bioorganic & Medicinal Chemistry 12 (2004) 2021–2034
Bioorganic & Medicinal Chemistry

Exploring distal regions of the A_3 adenosine receptor binding site: sterically constrained N^6-(2-phenylethyl)adenosine derivatives as potent ligands

Susanna Tchilibon, Soo-Kyung Kim, Zhan-Guo Gao, Brian A. Harris, Joshua B. Blaustein, Ariel S. Gross, Heng T. Duong, Neli Melman and Kenneth A. Jacobson*

Molecular Recognition Section, Laboratory of Bioorganic Chemistry, National Institute of Diabetes & Digestive & Kidney Diseases, National Institutes of Health (NIH), DHHS, Bethesda, MD 20892-0810, USA

Received 13 December 2003; revised 11 February 2004; accepted 28 February 2004

Abstract—We synthesized phenyl ring-substituted analogues of N^6-(1*S*,2*R*)-(2-phenyl-1-cyclopropyl)adenosine, which is highly potent in binding to the human A_3AR with a K_i value of 0.63 nM. The effects of these structural changes on affinity at human and rat adenosine receptors and on intrinsic efficacy at the hA_3AR were measured. A 3-nitrophenyl analogue was resolved chromatographically into pure diastereomers, which displayed 10-fold stereoselectivity in A_3AR binding in favor of the 1*S*,2*R* isomer. A molecular model defined a hydrophobic region (Phe168) in the putative A_3AR binding site around the phenyl moiety. A heteroaromatic group (3-thienyl) could substitute for the phenyl moiety with retention of high affinity of A_3AR binding. Other related N^6-substituted adenosine derivatives were included for comparison. Although the N^6-(2-phenyl-1-cyclopropyl) derivatives were full A_3AR agonists, several other derivatives had greatly reduced efficacy. N^6-Cyclopropyladenosine was an A_3AR antagonist, and adding either one or two phenyl rings at the 2-position of the cyclopropyl moiety restored efficacy. N^6-(2,2-Diphenylethyl)adenosine was an A_3AR antagonist, and either adding a bond between the two phenyl rings (N^6-9-fluorenylmethyl) or shortening the ethyl moiety (N^6-diphenylmethyl) restored efficacy. A QSAR study of the N^6 region provided a model that was complementary to the putative A_3AR binding site in a rhodopsin-based homology model. Thus, a new series of high-affinity A_3AR agonists and related nucleoside antagonists was explored through both empirical and theoretical approaches.

1. Introduction

The adenosine receptors (ARs) consist of four subtypes (A_1, A_{2A}, A_{2B}, and A_3) and represent a physiologically important family of G protein-coupled receptors.[1] AR agonists are current targets for the development of therapeutic agents for a variety of diseases, including agents with neuroprotective, antiseizure, anti-inflammatory, anti-ischemic, and cardioprotective effects.[2–4] A_3AR agonists are also potentially useful for the treatment of cancer. In certain tumor cells, a cytostatic effect of the A_3AR agonist appears to be related to its downstream activation of the Wnt pathway.[5]

We have studied the microscopic interactions of ligands with the A_3AR and other members of the AR family from the perspectives of both ligand modification and structure–function aspects of the receptors.[6–9] Extensive mutagenesis studies and molecular modeling based on a high-resolution template of rhodopsin have implicated TM (transmembrane domain) regions 3, 6, and 7 in the coordination of adenosine agonists and a putative rotation of TM6 in the activation of the A_{2A} and A_3ARs.

Adenosine is a nonselective AR agonist that is rapidly degraded in circulation. Its clinical use for treatment of supraventricular tachycardia is predicated on a short duration of action. However, other foreseeable applications of synthetic adenosine agonists would require greater stability in vivo.[10] An early AR agonist showing improved stability toward adenosine deaminase was the nonselective agonist 2-chloroadenosine **1**, which also served as the first stable adenosine receptor radioligand.[11]

Keywords: Nucleoside; Agonist; Molecular modeling; GPCR; Purine receptor.
* Corresponding author. Tel.: +301-496-9024; fax: +301-480-8422; e-mail: kajacobs@helix.nih.gov

0968-0896/$ - see front matter © 2004 Elsevier Ltd. All rights reserved.
doi:10.1016/j.bmc.2004.02.037

The 2-chloro modification has since been incorporated in many potent AR agonists, including the 5′-uronamide derivative Cl-IB-MECA **2**, the first highly selective A_3AR agonist. The intrinsic efficacy of various adenosine derivatives as A_3AR agonists was studied, leading to the characterization of structure–activity relationships (SARs) for efficacy, which are distinct from those of affinity.[6,7] The ability of a tightly binding adenosine derivative to activate the A_3AR is highly dependent on ligand conformation. The flexibility of the ribose moiety has been established as a required feature for A_3AR agonists. Steric constraint of the ribose moiety, for example, the introduction of a bridged carbocyclic ring system, tends to reduce intrinsic efficacy of the adenosine derivatives at the human A_3AR (hA_3AR). These effects are overridden by the presence of a flexible 5′-uronamide group.

Highly selective A_3AR agonists thus far reported, for example, **2** (2-chloro-N^6-(3-iodobenzyl)-5′-*N*-methylcarboxamidoadenosine), all contain multiple substitutions of the adenosine molecule.[1] A recent study by Gao et al.[7] identified the singly substituted adenosine derivative compound **3** (N^6-(1*S*,2*R*)-(2-phenyl-1-cyclopropyl)adenosine), with a K_i value in binding to the hA_3AR of 0.63 nM (38-fold more potent than the 1*R*,2*S* isomer **4**), as a lead for the development of N^6 derivatives of adenosine with high hA_3AR affinity. The present study aimed to identify analogues of **3** and other N^6 derivatives of adenosine that are selective, while maintaining the remainder of the molecule unchanged, and to categorize structural features of the N^6 substituents that affect the intrinsic efficacy (Chart 1).

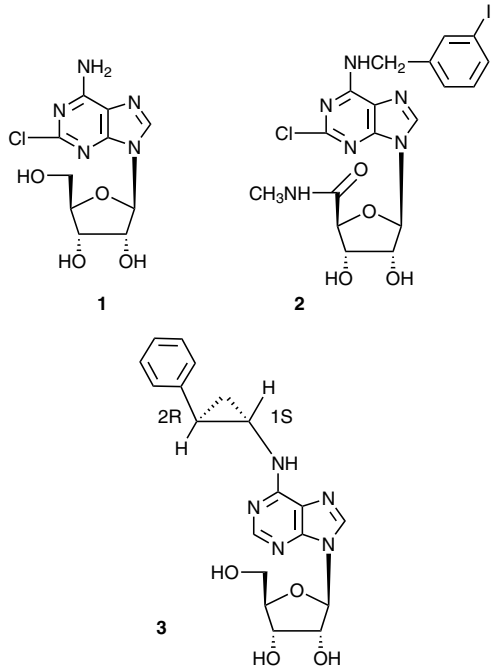

Chart 1. The structure of the various adenosine agonists studied at the A_3AR.

2. Results

2.1. Chemical synthesis

Most of the analogues of **3** were prepared as diastereomeric mixtures (Schemes 1–3). The phenylcyclopropyl amines **41a**–**n** were prepared from the corresponding *trans*-cinnamic acid derivatives **37**.[12] With the exception of the 3-cyano-cinnamic acid (**37k**), which was obtained by a Knövenagel condensation between 3-cyano-benzaldehyde and malonic acid, the other acids were commercially available.

After esterification with methanol in the presence of H_2SO_4, compounds **38a**–**n** were cyclopropanated with diazomethane in the presence of catalytic $Pd(OAc)_2$. This is a very high-yield reaction with the only inconvenience being that it must be monitored by NMR, because the starting material and product were undistinguishable by TLC. Hydrolysis of the esters **39a**–**n** gave the desired *trans*-arylcyclopropanecarboxylic acids **40a**–**n**. The primary amines **41a**–**n** were obtained by a Curtius degradation, in a one-pot reaction with diphenyl phosphorazidate, with the exception of **44** and **45** (Scheme 2). For these two compounds a two-step reaction with sodium azide was preferred, because in this way the resulting acyl azides were transformed into the 2-(trimethylsilyl)ethyl carbamate, which could be hydrolyzed with tetrabutylammonium fluoride without affecting the acetamido moiety. A diphenylcyclopropyl intermediate, the carboxylic acid **47**, was prepared by the method reported (Scheme 3).[21] In this case the cyclopropanation of 3-phenyl-cinnamic acid was unsuccessful, probably because of the steric hindrance. Once obtained, the amines **41**, **44a**–**n**, **45**, and **48** reacted with 6-chloropurine riboside to give the desired adenosine analogues **6**–**15** and **19**–**25**. Compound **18** was obtained by simple hydrogenation on Pd/C of the nitro derivative **15**.

One of the analogues, containing a 3-nitro group (**15**), was resolved into pure diastereomers with HPLC, using the chiral column Chiralpak AD. The assignment of absolute configuration was done by analogy to the unsubstituted phenylcyclopropyl derivatives as standards.[7] In the condition used for the chiral separation, the pure N^6-[(1*R*,2*S*)-2-phenyl-1-cyclopropyl]adenosine (**4**) showed a retention time of 10.1 min and N^6-[(1*S*,2*R*)-2-phenyl-1-cyclopropyl]adenosine (**3**) of 13.3 min. By analogy, in the resolution of the racemic **15**, the first eluting peak at the retention time of 20.8 min was assigned as the N^6-[(1*R*,2*S*)-2-(3-nitrophenyl)-1-cyclopropyl]adenosine (**17**) and the later one at 31.5 min as N^6-[(1*S*,2*R*)-2-(3-nitrophenyl)-1-cyclopropyl]adenosine (**16**).

3. Biological activity

The analogues **5**–**25** of N^6-(*trans*-2-phenyl-1-cyclopropyl)adenosine (Table 1) generally bound to the hA_3AR in the low nanomolar range. Selectivity was high when

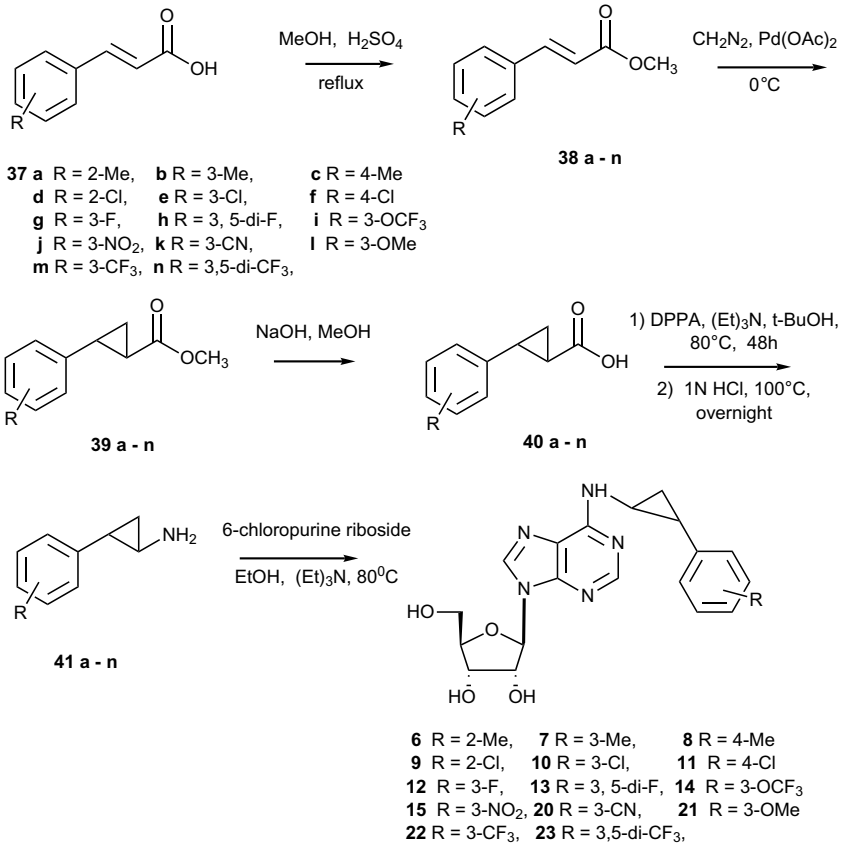

Scheme 1. General synthetic route used to prepare N^6-(2-phenyl-1-cyclopropyl)adenosine analogues.

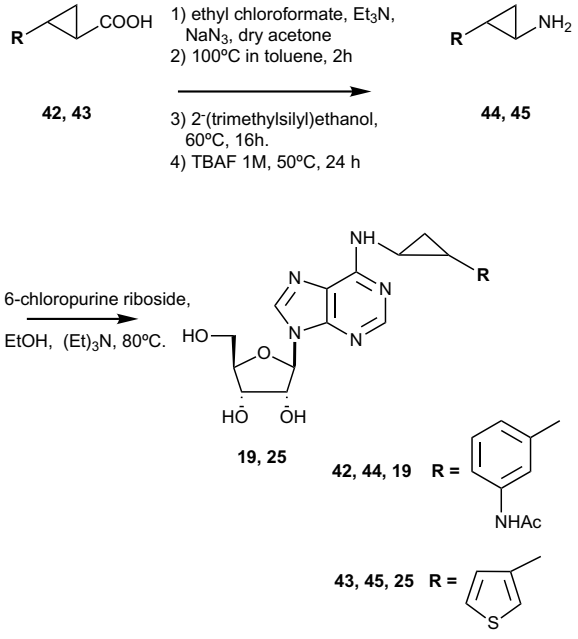

Scheme 2. Synthetic route used to prepare compounds **19** and **25** via a trimethylsilylethyl intermediate.

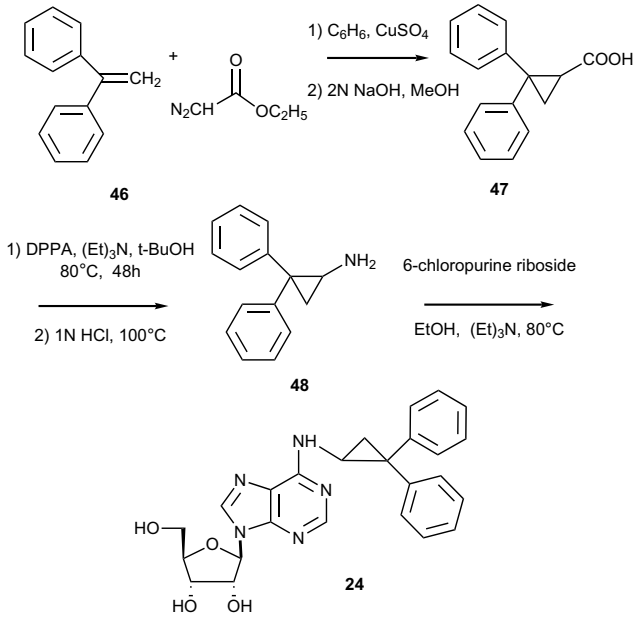

Scheme 3. Synthetic route used to prepare N^6-(2,2-diphenyl-1-cyclopropyl)adenosine **24**.

compared with the A_{2A}ARs, but only moderate, at most, compared with the A_1ARs. The diastereomeric mixture of N^6-(*trans*-2-phenyl-1-cyclopropyl)adenosine **5** was prepared for comparison with the phenyl-substituted analogues. Compound **5** bound to the hA_3AR with a K_i value of 0.86 nM. Its affinity at the rat A_3AR (rA_3AR) was 460-fold lower than at the human receptor. Substitution of the 2-phenyl ring at the 3-position was

Table 1. Binding affinities of adenosine derivatives at human and rat A_1, A_{2A}ARs and A_3ARs and maximal agonist effects at the hA_3AR expressed in CHO cells.[a] The adenosine derivatives are substituted at the N^6 position as indicated. Compounds **1** and **2** are additionally substituted at the 2-position with chloro. All compounds except **2** are simple 9-β-D-riboside derivatives

#	N^6 substitution	K_i (nM)					Maximum effect (%)[d]
		rA_1AR[a]	$rA_{2A}AR$[b]	hA_1AR[a]	$hA_{2A}AR$[b]	hA_3AR, h or (r)[c]	
trans-N^6-(2-Phenyl-1-cyclopropyl) analogues							
3	(1*S*,2*R*)-2-Phenyl-1-cPr	11.8 ± 2.4[e]	560 ± 232[e]	30.1 ± 6.1	2250 ± 430	0.63 ± 0.17[e] (358 ± 33)[e]	117 ± 9
4	(1*R*,2*S*)-2-Phenyl-1-cPr	15.2 ± 3.2[e]	3040 ± 490[e]	15.6 ± 1.7	2340 ± 330	24.1 ± 10.9[e] (694 ± 157)[e]	87 ± 4
5	2-Phenyl-1-cPr	10.4 ± 1.9	2980 ± 310	124 ± 30	2530 ± 720	0.86 ± 0.09 (399 ± 28)[e]	101 ± 5
6	2-(2-Methylphenyl)-1-cPr	18.3 ± 3.3	1080 ± 250	116 ± 19	4480 ± 460	12.9 ± 3.9	98 ± 4
7	2-(3-Methylphenyl)-1-cPr	17.3 ± 2.9	2500 ± 550	12.1 ± 2.7	970 ± 340	1.59 ± 0.50	107 ± 11
8	2-(4-Methylphenyl)-1-cPr	20.0 ± 1.9	2760 ± 970	28.0 ± 3.4	3130 ± 710	1.96 ± 0.14	99 ± 7
9	2-(2-Chlorophenyl)-1-cPr	11.8 ± 1.5	1430 ± 330	28.4 ± 13.7	1820 ± 170	6.0 ± 1.4	104 ± 6
10	2-(3-Chlorophenyl)-1-cPr	10.3 ± 1.1	349 ± 56	24.9 ± 2.1	1520 ± 540	0.98 ± 0.27 (642 ± 153)	101 ± 3
11	2-(4-Chlorophenyl)-1-cPr	9.70 ± 2.73	1430 ± 540	79.5 ± 41.0	4120 ± 890	1.63 ± 0.26	103 ± 7
12	2-(3-Fluorophenyl)-1-cPr	13.6 ± 1.7	1410 ± 750	35.1 ± 8.3	2930 ± 330	7.6 ± 1.4	110 ± 12
13	2-(3,5-Difluorophenyl)-1-cPr	18.8 ± 1.8	4060 ± 1330	39.7 ± 4.0	3270 ± 700	34.7 ± 3.1	99 ± 8
14	2-(3-Trifluoromethyloxyphenyl)-1-cPr	36.3 ± 9.9	1360 ± 230	146 ± 63	7110 ± 930	77.3 ± 21.3	97 ± 6
15	2-(3-Nitrophenyl)-1-cPr	15.4 ± 2.8	1060 ± 260	47.5 ± 0.5	2260 ± 270	18.8 ± 5.2	100 ± 5
16	2-(3-Nitrophenyl)-1-cPr, B (1*S*,2*R*)	13.6 ± 3.2		83.9 ± 8.2	>10,000	11.2 ± 2.7	108 ± 4
17	2-(3-Nitrophenyl)-1-cPr, A (1*R*,2*S*)	13.2 ± 4.6		55.4 ± 7.8	1320 ± 370	116 ± 13	64 ± 7
18	2-(3-Aminophenyl)-1-cPr	46.9 ± 7.8	8040 ± 1380	131 ± 52	>10,000	9.0 ± 3.3	103 ± 7
19	2-(3-Acetamidophenyl)-1-cPr	21.5 ± 9.4		32.6 ± 7.5	2130 ± 700	6.02 ± 0.74	100 ± 9
20	2-(3-Cyanophenyl)-1-cPr	57.4 ± 5.8	2450 ± 610	45.2 ± 3.3	2480 ± 780	22.5 ± 7.5	99 ± 7
21	2-(3-Methoxyphenyl)-1-cPr	15.8 ± 1.4	795 ± 193	29.1 ± 5.9	2830 ± 340	2.8 ± 0.3	103 ± 2
22	2-[3-(Trifluoromethyl)phenyl]-1-cPr	15.6 ± 1.6	459 ± 97	104 ± 30	2370 ± 780	1.9 ± 0.2	101 ± 5
23	2-[3,5-Di(trifluoromethyl)phenyl]-1-cPr	46.1 ± 6.7	869 ± 351	40.7 ± 2.4	7660 ± 1040	387 ± 37	98 ± 8
24	2,2-Diphenyl-1-cPr	22.6 ± 8.7	54.6 ± 17.6	71 ± 15	579 ± 186	91 ± 14	100 ± 4
25	2-(3-Thienyl)-1-cPr	5.65 ± 1.97		31.6 ± 8.2	2120 ± 670	2.88 ± 0.90	99 ± 7
Other analogues							
1	CADO	6.7 ± 1.0[f]	63[e]	7.5 ± 1.4	630 ± 220	87 ± 24 (1890 ± 900)[g]	100 ± 7[e]
2	3-Iodobenzyl, Cl-IB-MECA	820[e]	470[e]	1240 ± 320[h]	5360 ± 2470[h]	1.4 ± 0.3[h] (0.33)[e]	100
26	Benzyl	175 ± 20[e]	285[e]	77.8 ± 6.5	2180 ± 670	41.3 ± 5.3[e] (120 ± 20)[g]	55 ± 3
27	2-Phenylethyl	24.0 ± 8.8[f]	521 ± 90	12.9 ± 2.1	676 ± 39	2.1 ± 0.4 (240 ± 58)[g]	84 ± 5
28	(*R*)-1-Phenyl-2-propyl, (*R*)-PIA	1.2 ± 0.1[f]	124[f]	2.04[i]	859[i]	8.7 ± 0.9[e] (158)[g]	102 ± 6[e]
29	(*S*)-1-Phenyl-2-propyl, (*S*)-PIA	49.3[f]	1820[f]	75[i]	7780[i]	68 ± 12[e] (920)[g]	97 ± 3[e]
30	(*R*)-2-Phenyl-1-propyl	1.4 ± 0.1[e]	319 ± 114	4.0 ± 1.3	325 ± 85	9.1 ± 0.3 (202 ± 20)	99 ± 4
31	(*S*)-2-Phenyl-1-propyl	3.5 ± 0.3[e]	459 ± 162	26.6 ± 6.8	1120 ± 260	38.8 ± 4.1 (276 ± 20)	98 ± 6
32	Cyclopropyl	14.7 ± 1.7	3490 ± 260	6.9 ± 2.4	7860 ± 550	100 ± 33 (1950 ± 120)	0[j]
33	2,2-Diphenylethyl	44.1 ± 1.7	75.4 ± 14.9	49.9 ± 16.2	510 ± 49	3.9 ± 0.7 (538 ± 202)	0[j]
34	2-(3,5-Dimethoxyphenyl)-2-(2-methylphenyl)ethyl, DPMA	112 ± 49	4.4[g]	168 ± 29[e]	153 ± 26[e]	106 ± 22[e] (3570 ± 1700)[g]	0[e]
35	Diphenylmethyl	208 ± 36	2490 ± 420	490 ± 242	>10, 000	3340 ± 360	87 ± 6
36	9-Fluorenylmethyl	9.41 ± 3.11	33.4 ± 24.4	14.0 ± 4.0	145 ± 26	0.91 ± 0.38	99 ± 6

[a] Binding experiments at rat brain and recombinant human A_1ARs used [^{3}H]R-PIA (2.0 nM) as radioligand, unless noted.
[b] Binding experiments at rat brain and recombinant human A_{2A}ARs used [^{3}H]CGS21680 (15 nM) as radioligand, unless noted.
[c] All A_3AR binding experiments were performed using adherent CHO cells stably transfected with cDNA encoding the human or rat A_3 receptor. [^{125}I]I-AB-MECA was used as radioligand.
[d] Data of hA_3AR at 10 μM. Functional assay consisting of inhibition of forskolin-stimulated adenylyl cyclase. The value for compound **2** is the standard for 100% efficacy.
[e] Data from Gao et al.[7]
[f] Data from Daly et al.[14]
[g] Data from van Galen et al.[23]
[h] Data from Jacobson et al.[24]
[i] Data from Klotz et al.[25] Radioligands used were [^{3}H]CPX and [^{3}H]NECA at human A_1 and A_{2A} ARs, respectively.
[j] When the stock DMSO solution was subjected to repeated freeze-thaw cycles, the observed efficacy was affected. Values given are for freshly prepared solutions.

favorable for hA_3AR affinity. Thus, among the methyl-substituted analogues **6**–**8**, the most potent in A_3AR binding was the 3-methyl analogue **7**. Similarly, within a series of chloro-substituted analogues **9**–**11**, the order of potency in binding was 3-Cl > 4-Cl > 2-Cl. The 3-chloro analogue **10** bound to the hA_3AR with a K_i value of 0.98 nM, and the affinity at the rA_3AR was 660-fold lower. Thus, there were dramatic species differences in affinity, and A_3AR selectivity of **10** was present when comparing human but not rat ARs. At rARs, compound **10** was moderately selective for the A_1AR.

The 3-fluoro analogue **12** was 8-fold less potent than **10** at the hA_3AR. 3,5-Difluoro or 3-trifluoromethyl oxy substitution, in **13** and **14**, respectively, further lowered the affinity. The 3-nitro analogue **15** displayed A_3AR selectivity of 120-fold compared with the $hA_{2A}AR$. The two isomers of this diastereomeric mixture, **16** and **17**, differed 10-fold in A_3AR affinity. The more potent 1*S*,2*R* analogue **16** was >900-fold selective for the hA_3 compared with $hA_{2A}AR$. The corresponding 3-amino analogue **18** was 9-fold weaker than **15** at the hA_3AR. This 3-amino derivative also displayed decreased affinity at the human and rat A_{2A} ARs. The 3-acetamido derivative **19** was more potent than the corresponding 3-amino derivative at all subtypes. Another electron-withdrawing group, 3-cyano in compound **20**, did not provide high affinity, but an electron-donating group, 3-methoxy in **21**, resulted in high A_3AR affinity. The analogue **22**, which contains an electron-withdrawing 3-trifluoromethyl group, bound to the hA_3AR with high affinity. However, two 3-trifluoromethyl groups in **23** greatly reduced the affinity at the A_3AR. The 2,2-diphenylethyl substituted analogue **24** was not highly potent at the A_3AR and was generally nonselective. However, a heteroaromatic group could be substituted in the place of the phenyl moiety of compound **5**; thus, a 2-(3-thienyl) analogue **25** displayed high A_3AR affinity.

For comparison, a number of previously reported analogues were studied in the same assays. The N^6-benzyl group has been widely explored in the design of A_3AR agonists, such as Cl-IB-MECA **2**. The combination of N^6-(3-iodobenzyl) and 5′-uronamido groups in **2** greatly enhanced both the A_3AR potency and the selectivity in comparison to **1**. However, the simple 2-H benzyl derivative **26** was only 2-fold more potent at the hA_3AR than **1**. The next higher homologue, the 2-phenylethyl derivative **27**, was of greatly increased affinity and selectivity at the human (but not rat) A_3AR. Branching of the alkyl groups in N^6-substituted adenosines has been well studied at the A_1AR and $A_{2A}AR$.[13–16] At the hA_3AR, a moderate degree of stereoselectivity of binding was observed for introduction of a methyl group in the R configuration at either the 1-(**28** compared with **29**) or 2-(**30** compared with **31**) position.

Although the cyclopropyl group of the N^6-(2-phenyl-1-cyclopropyl) analogues **3**–**25** was introduced for steric constraint, intended to freeze the biologically preferred conformation, these analogues could also be considered hybrids of the N^6-phenylethyl analogue **27** and the N^6-cyclopropyl analogue **32**. Compound **32**, however, was not highly potent in binding to the hA_3AR.

A functional assay of A_3AR-mediated inhibition of forskolin-stimulated adenylyl cyclase showed marked effects of certain N^6 substitution on intrinsic efficacy. The prototypical A_3AR agonist Cl-IB-MECA **2** is considered a full agonist in most studies,[1,6] although in calcium responses in monocyte-derived dendritic cells it appeared to be a partial agonist.[18] The efficacy of the analogues was reported as a single percentage value (relative to the full agonist **2**) at a nucleoside concentration of 10 μM. The efficacy at the hA_3AR of the N^6-(2-phenyl-1-cyclopropyl) analogues **3**–**25** was generally nearly full (i.e., 100%). In a full concentration-response experiment (Fig. 1), compound **10** was found to be a full agonist at the hA_3AR in the inhibition of adenylate cyclase. The functional potency of **10** was comparable to that of **2**. The functional EC_{50} values for both were ~3 nM, which is in agreement with the K_i values in binding of ~1 nM. In contrast, N^6-cyclopropyladenosine **32** appeared to be an antagonist, with lack of efficacy at 10 μM, at a concentration 100 times greater than its K_i value in binding at the hA_3AR. A N^6-(2,2-diphenylethyl) analogue **33** also proved to be an antagonist. A Schild analysis of inhibition by **33** of the effects of an A_3AR agonist at the hA_3AR was carried out (Fig. 2); it demonstrated that the K_B value for this competitive antagonist was 5.0 nM. This was consistent with the previously observed antagonist properties of the closely related DPMA **34** at the hA_3AR.[7] Shortening the ethyl moiety by one carbon, that is to obtain **35**, or constraining the two rings with a biaryl bond, that is **36**, largely restored efficacy, although the A_3AR affinity of these two compounds varied greatly. The 9-fluorenylmethyl analogue **36** was as potent at the hA_3AR as the most potent N^6-(2-phenyl-1-cyclopropyl) analogues in this study. Nevertheless, **36** displayed only minimal selectivity in comparison to the A_1AR.

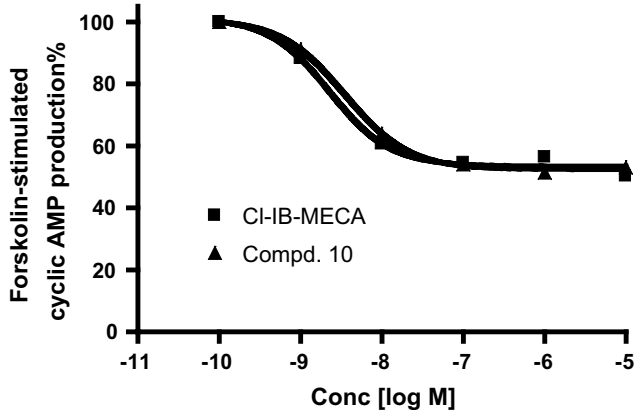

Figure 1. Effects of Cl-IB-MECA and **10** on cAMP production in CHO cells stably expressing the hA_3AR. The cAMP level corresponding to 100% (10 μM forskolin) was 220 ± 30 pmol mL^{-1}. The EC_{50} value for compound **10** was 3.7 ± 0.6 nM. Results are from a single representative experiment, which was carried out in triplicate.

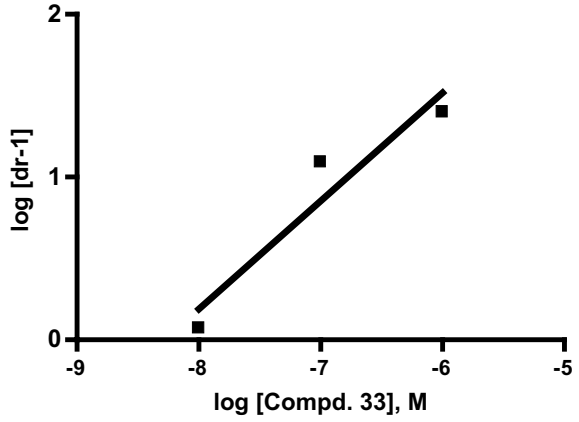

Figure 2. Antagonism by compound **33** of the inhibition of cyclic AMP production elicited by Cl-IB-MECA in CHO cells stably transfected with the hA_3AR. The experiment was performed in the presence of 10 μM rolipram and 3 units/mL adenosine deaminase. Forskolin (10 μM) was used to stimulate cyclic AMP levels. The level of cAMP corresponding to 100% was 220 ± 30 pmol mL^{-1}. The K_B value for compound **33** was calculated to be 5.0 nM.

The effect of selected compounds, at a single concentration of 10 μM, on stimulation of adenylyl cyclase via the $hA_{2B}AR$ in stably transfected CHO (Chinese hamster ovary) cells was examined. 5′-*N*-Ethyluronamidoadenosine (NECA) stimulated cyclic AMP accumulation in a concentration-dependent manner corresponding to an EC_{50} of 140 ± 19 nM ($n = 4$). The maximum stimulation level of NECA at 10 μM was expressed as 100%. Most compounds tested at 10 μM had only a small effect (<50%) on cyclic AMP accumulation. The ranges of percentage stimulation were 30–50% (**3**, **6**–**10**, and **15**), 15–30% (**5**, **11**, **12**, **17**, **19**, **25**, and **35**), <15% (**13**, **14**, **16**, **18**, **20**–**23**, and **31**). Compounds that stimulated to >50% of the NECA response were **4** (60 ± 2%), **24** (78 ± 2%), **30** (56 ± 3%), **34** (6 3 ± 8%), and **36** (96 ± 2%).

4. Molecular modeling

As the first step in modeling the environment within the hA_3AR surrounding the distal portion of the N^6-binding region, the agonist template molecule N^6-(1*S*,2*R*)-(2-phenyl-1-cyclopropyl) adenosine **3** was docked in a rhodopsin-based homology model of the receptor.[8] We used the previously reported Cl-IB-MECA/hA_3AR complex as the starting geometry for the position of the ribose moiety of **3**, followed by a systematic conformational search varying the rotatable bonds of the N^6 substitutent, that is t_0 (C_5–C_6–N_6–C_{cp}) and t_1 (C_6–N_6–C_{cp}–C_{cp}) angles. The constraint of the cyclopropyl ring fixed the t_2 (N_6–C_{cp}–C_{cp}–C_{ar}) torsion angle. The energetically optimized result of docking **3** in the hA_3AR is shown in Figure 3. Mutagenesis results were consistent with molecular modeling that featured direct interaction of nucleosides with TMs 3, 6, 7, and EL2 (the second extracellular loop).[6,8,30] Residues that were within 5 Å proximity to **3** in this putative binding site were L91 (3.33), T94 (3.36), H95 (3.37), N150 (EL2), Q167 (EL2),

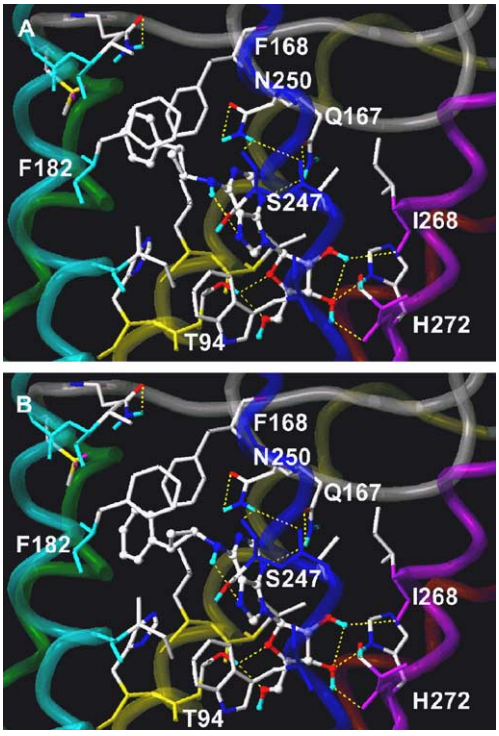

Figure 3. The complex of the A_3AR with two regioisomers in the putative binding site of the hA_3AR model. (A) (1*S*,2*R*)-2-phenyl-1-cyclopropyl-adenosine **3** and (B) (1*R*,2*S*)-2-phenyl-1-cyclopropyl-adenosine **4**. All ligands are displayed as ball and stick models, and the side chains of hA_3AR are shown as stick models. The H-bonding between ligand and hA_3AR is displayed in yellow. The A_3AR is represented by a tube model with a different color for each TM domain (TM3 in yellow, TM4 in green, TM5 in cyano, TM6 in blue, TM7 in purple).

F168 (EL2), S181 (5.42), M177 (5.38), V178 (5.39), F182 (5.43), F239 (6,44), W243 (6.48), L246 (6.51), S247 (6.52), N250 (6.55), I268 (7.39), S271 (7.42), H272 (7.43), and N274 (7.45). For comparison, the less potent isomer **4** was docked in a similar manner.

The purine ring of **3** was located in a hydrophobic pocket defined by L91 (3.33) and L246 (6.51). The amine of the N^6 substituent in proximity to N250 (6.55) was H-bonded with the hydroxyl group of S247 (6.52), and the purine N^3 atom formed an H-bond with the side chain of Q167 (EL2). The 2′-OH group of the ribose ring was involved in H-bonding with the backbone carbonyl group of I268 (7.39), and the 3′-OH group formed H-bonds with the carbonyl group of the backbone of S271 (7.42) and the side chain of H272 (7.43), consistent with our A_3 neoceptor model.[31] The 5′-hydroxyl group also formed an H-bond with T94 (3.36). The phenyl moiety showed an additional hydrophobic interaction with F168 (EL2). Compared with the Cl-IB-MECA complex, in the case of N^6-phenylcyclo propyladenosine, the phenyl ring showed a better π–π stacking interaction with the aromatic ring of F168 (EL2). The distances between the centers of the N^6-phenyl ring and the F168 aromatic ring were 3.69, 4.55, and 4.21 Å, for compounds **3**, **4**, and Cl-IBMECA, respectively. Thus, the 1*S*,2*R* isomer **3** showed a better π–π stacking interaction

than **4** in the distal region of the binding site of the N^6 substituent, consistent with its higher measured binding affinity.

The docked conformation of **3** displayed a preference for t_0, t_1, and t_2 angles of approximately −110°, −80°, and 140°, respectively, in the docking complex of **4** the angles of t_0, t_1, and t_2 were −130°, 80°, and −140°. Thus, the preferred t_1 and t_2 angles differed between the two diastereomers. The **3**-hA_3AR complex showed ∼5 kcal lower energy than that of the agonist **4**, correlating with the binding affinity. The binding affinity of **3** was ∼40-fold higher than that of **4**. The relative stability of the hA_3AR complex with the nitrophenyl diastereomer N^6-(1*S*,2*R*)-(2-phenyl-1-cyclopropyl) adenosine **16** and its less potent 1*R*,2*S* diastereomer **17** was also checked. The receptor complex of **16** showed ∼1.4 kcal lower energy than the complex of **17**, consistent with the stereoselectivity of binding at the hA_3AR. Thus, the docking study of the hA_3AR suggested that the 1*S*,2*R* diastereomer might show more favorable enthalpy of binding to the hA_3AR compared with the 1*R*,2*S* isomer, thus increasing the binding affinity.

The adenosine analogues with substitution of the phenyl ring of the N^6 substituent displayed a more limited rotational freedom of this ring when docked in the hA_3AR.[32] The 1*S*,2*R* diastereoisomers were assumed to be generally more potent and therefore were used in the docking. The phenyl substituents tended to be directed toward EL2, especially residue N150. However, the docked complexes of **15** and **18** showed different locations of the nitro and amino groups of the phenyl ring, that is directed toward TM4 and TM5 rather than EL2, because of more favorable nonbonding van der Waals interactions, while keeping the same preference of t_0, t_1, and t_2 angles as for other phenyl substitutions.

All ligands in Table 1 were subjected to similar receptor docking, and binding energies were calculated. The relative binding energies for analogues substituted on the phenyl moiety at the *ortho*, *meta*, and *para* positions were 4.0, 0, and 1.4 kcal for a Cl atom, and 1.3, 0, and 0.3 kcal for a methyl group. For both substituents, receptor docking confirmed that the *meta* position was the most and the *ortho* position was the least energetically favorable for binding to the hA_3AR, and this would be consistent with the experimental results.

Following the initial receptor docking of the set of N^6-modified adenosine derivatives, 3D-QSAR (quantitative structure activity relationship) studies were performed with CoMFA (comparative molecular field analysis)[34,35] and CoMSIA (comparative molecular similarity indices analysis).[36] Two distinct models for the training set in 3D-QSAR, 1 and 2 as defined in the experimental section,[33] were derived by superimposition of the complexes in which the ligands were docked in the putative binding site of the hA_3AR. The results were compared according to the two models (Table 2). PLS (partial least squares) analysis of model 1 generated in the CoMFA 3D-QSAR model displayed a modest q^2 value of 0.44 and an r^2 value of 0.98 for 27 compounds only after removing five compounds (**1**, **10**, **15**, **18**, and **29**). These compounds were detected as outliers from the residual plot of the leave-one-out cross-validation. Model 2, with a similar 3D orientation to the docking study, generated a better 3D-CoMFA result than did model 1. This model displayed a q^2 value of 0.57 and an r^2 value of 0.97, for 29 out of 32 compounds. Fewer compounds (**13**, **21**, and **32**) were outliers in model 2 than in model 1.

CoMSIA methods with additional hydrophobic and H-bonding fields[37] have been shown to be of comparable statistical significance to traditional CoMFA models, but with somewhat more easily interpreted isocontour surface maps. Here, CoMSIA performed better than CoMFA. The better statistical result of CoMSIA was attributed to the large contributions of hydrophobic and H-bonding interactions (Table 2). In addition, the conformational diversity, using model 1 for 3D-QSAR, did not affect any statistical parameters of CoMSIA, whereas CoMFA was very sensitive to the conformation used for the model. Both CoMSIA models required two different outliers to reach the predictable model with a q^2 value of >0.4. The result of the CoMSIA model was a q^2 value of 0.53 for model 1 and a q^2 value of 0.47 for model 2 with the same r^2 value of 0.96 for both models.

The superimposition of the CoMFA/CoMSIA map onto the binding site of the receptor was interpretable with respect to the SAR, because all conformations of the

Table 2. The result of CoMFA and CoMSIA 3D-QSAR for two models

Statistics	CoMFA		CoMSIA	
	Model 1	Model 2	Model 1	Model 2
q^2	0.44	0.57	0.53	0.47
Number of compounds	27	29	30	30
Number of components	5	6	6	6
r^2	0.98	0.97	0.96	0.96
SEE[a]	0.13	0.16	0.18	0.19
F	198	124	99	87
Contribution (%)				
Steric	59.70	60.80	10.10	10.70
Electrostatic	40.30	39.20	30.60	38.90
Hydrophobic			28.30	31.20
H-bond donor			24.80	15.10
H-bond acceptor			6.20	4.20

[a] Standard error of estimate.

two models used for 3D-QSAR analyses were obtained from the docking complex without any modifications, such as RMS fitting and database alignment with a template. The CoMFA and CoMSIA maps of the two models showed similar contour maps for steric, electrostatic, hydrophobic, and H-bonding fields, except for the contours representing regions of hydrophilicity and disfavored steric bulk (data not shown). The best contour maps for each property through the correlation with the binding site environment were the steric and the electrostatic maps from the CoMFA model 2 and the hydrophobic and H-bonding maps from the CoMSIA model 1 (Fig. 4). The projection of the CoMFA/CoMSIA contour maps onto the binding site, which was validated by the experimental results, displayed a good complementarity. As shown in Figure 4B, blue regions, indicating that an electropositive group would increase the affinity, were located near the *meta* position of the phenyl group (V141 (4.56), N150 (EL2)) and surrounding the adenine ring (N250 (6.55), Q167 (EL2), T94 (3.36)). The interpretation of the existence of two blue contour maps at the *meta* position of the phenyl ring was that most of the electron-withdrawing groups with a negative charge did not improve the binding affinity compared with the unsubstituted compound **3**. A red CoMFA contour favoring a negatively charged group at the *para* position of the N^6-phenyl ring binding site was in proximity to S181 (5.42). For the steric CoMFA map in Figure 4A, a large green contour indicating tolerance of steric bulk around the N^6-phenyl group matched well with the hydrophobic binding site surrounded by F168 (EL2), M177 (5.38), and F182 (5.43). The green contour of CoMFA also coincided closely with the contour region of CoMSIA favoring hydrophobicity. Model 1 with the conformational diversity showed more regions of disfavored steric bulk in CoMFA and favored hydrophilic groups in CoMSIA than did model 2 (Fig. 4C). One of the hydrophilic contours from CoMSIA overlapped well with the less bulky contours from CoMFA. The H-bonding field map (Fig. 4D) was very useful because of the importance of H-bonding of adenosine analogues in binding to the hA_3AR, especially at the ribose-binding position and at the exocyclic amine of the adenine moiety. Because the

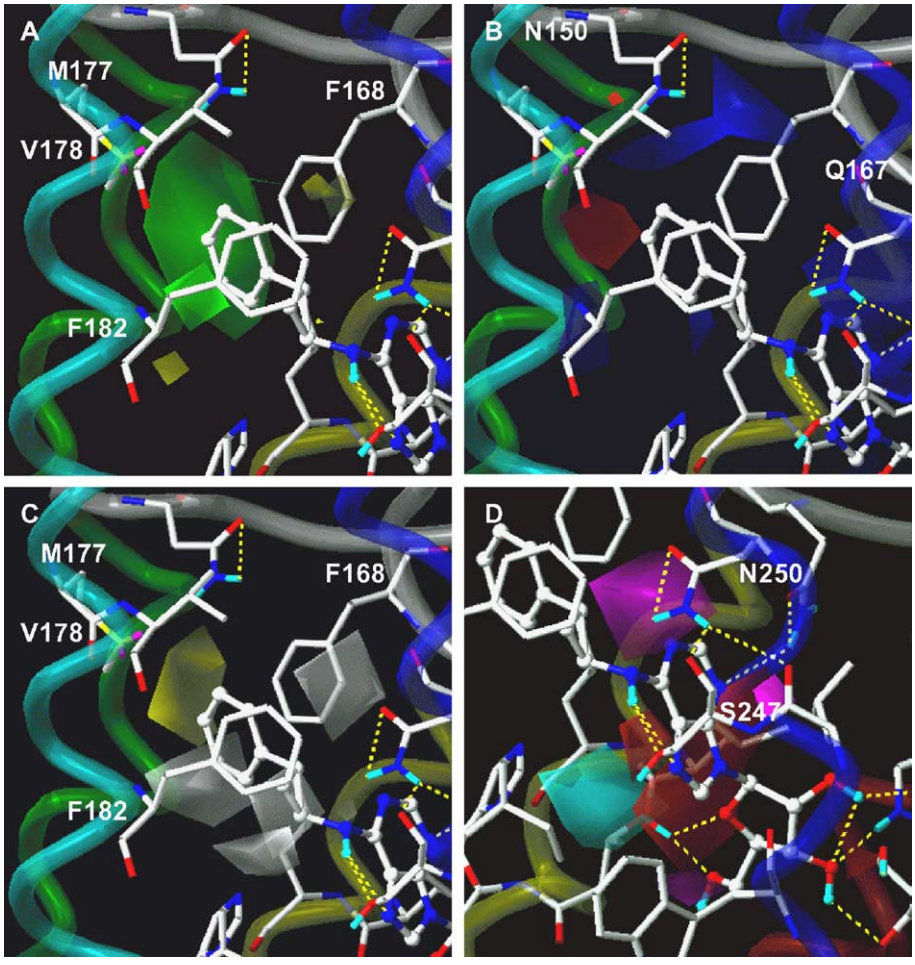

Figure 4. CoMFA stddev * coeff contour plots for model 2 (Top) and CoMSIA stddev * coeff contour plots for model 1 (bottom). (A) Predicted effects of structural modification on the binding affinity of **3** as docked in the hA_3AR: green contours indicate sterically favored regions; yellow contours indicate sterically disfavored regions. (B) Blue contours define a region where increased positive charge will result in increased affinity, and red contours define a region where increased negative charge will be favorable. (C) To enhance the binding affinity of hA_3AR, yellow and white areas define hydrophobic and hydrophilic preferences, respectively. (D) The H-bond donor field contour display regions where H-bond acceptors on the ligand are predicted to enhance (cyan) and disfavor (purple) binding. For the H-bond acceptor field, H-bond donors on the ligand are predicted to enhance (magenta) and disfavor (red) binding.

ribose ring was the core moiety, H-bonding fields were detected only near the N^6 and 5′-position. An H-bonding donor contour around the N^6 position was located at the side chain of S247 (6.52), and an H-bond acceptor contour around the N^6 position was directed toward the side chain of N250 (6.55). Thus, the steric, electrostatic, hydrophobic, and H-bonding contour maps were supported by the docking complex, with each contour map matched well with its surrounding amino acids with hydrophobic, hydrophilic, and H-bonding properties in the putative binding site of hA_3AR.

5. Discussion

CoMFA/CoMSIA 3D-QSAR and docking studies were conducted on a series of potent, conformationally constrained A_3AR agonists. The CoMFA/CoMSIA maps from the 3D-QSAR study and the putative binding site, based on both experimental results and a docking study, were integrated to propose a binding mode for hA_3AR agonists. The superimposition of the contour map from the CoMFA/CoMSIA study and the hA_3AR docking complex validated each other for the predictability of the ligand-based method as a 3D-QSAR and receptor-based approach through a homology modeling and docking study.

The molecular modeling studies of the A_3AR[6] indicate that required flexibility of the ribose moiety and a movement of TM6 were correlated with receptor activation. Similarly, at the $A_{2A}AR$ a rotation of a conserved Trp of TM6 has been proposed to be involved in activation.[8] We have assembled this series of adenosine derivatives to apply a similar analysis of SAR to the N^6 region.

The present study focused on derivatives of N^6-(2-phenylethyl)adenosine, in which various degrees of rigidity (a cyclopropane ring) and steric bulk (e.g., methyl groups of **28**–**31**) were included. The strikingly high affinity of the N^6-(1*S*,2*R*)-2-phenyl-1-cyclopropyl analogue **3** was further explored through phenyl ring substitution. None of the diastereomeric analogues proved to be more potent and selective than **3**, although moderate selectivity (**22**) and high affinity at the hA_3AR (**7**, **8**, **10**, **11**, **21**, **22**, and **25**) were achieved. The consistently greater affinity of these analogues at human compared with rat A_3ARs was also characteristic of the unsubstituted compounds **3** and **4** and the parent N^6-(2-phenylethyl)adenosine **27**.

Curiously, although the 2-phenyl-1-cyclopropyl analogues tended to be full agonists, several related derivatives had greatly reduced efficacy. The N^6-cyclopropyl derivative **32** was an A_3AR antagonist; adding one or two phenyl rings at the 2-position restored efficacy. The N^6-(2,2-diphenylethyl) derivative was a somewhat selective A_3AR antagonist, but either adding a bond between the two phenyl rings (N^6-9-fluorenylmethyl) or shortening the ethyl moiety (N^6-diphenylmethyl) restored efficacy. Thus, extending earlier findings,[6,7] the ability of an adenosine derivative to activate the A_3AR is highly dependent on the nature of the N^6 substituent. A new series of high-affinity A_3AR agonists and related nucleoside antagonists was explored, and ligand docking in a molecular model of the hA_3AR defines a hydrophobic region for interaction with the N^6-(2-phenylethyl) moiety. These findings for the N^6 region may be combined synthetically with other structural modifications to enhance the pharmacological profile for either A_3AR selectivity or mixed A_1/A_3AR selectivity. Agonists of mixed A_1/A_3AR selectivity may be useful for treating cardiac ischemia.[22] To investigate the structural basis for the differences in affinity between species and the striking variation in intrinsic efficacy will require the use of receptor mutagenesis.[6,8]

6. Conclusion

A new series of high-affinity A_3AR agonists was explored. The adenosine derivatives are mainly sterically constrained analogues of N^6-(2-phenylethyl)adenosine, found previously to display high affinity at the hA_3AR. The affinity and selectivity of these nucleosides is highly dependent on the species examined and on the substitution of a distal aryl substitution. A molecular model defines a hydrophobic region, which includes Phe168 of EL2, in the putative A_3AR binding site around the distal phenyl moiety. Upon probing of the SAR in this series, several novel nucleoside antagonists of the A_3AR were identified.

7. Experimental

7.1. Chemistry

7.1.1. Materials and instrumentation. Reagents and solvents were purchased from Sigma–Aldrich (St. Louis, MO). ^1H NMR spectra were obtained with a Varian Gemini 300 spectrometer using $CDCl_3$ as a solvent. The chemical shifts are expressed as ppm downfield from TMS. High-resolution FAB mass spectrometry was performed with a JEOL SX102 spectrometer using 6 kV Xe atoms. The chiral separation was done with a Hewlet Packard 1090 HPLC system using a Chiralpak AD column at an isocratic method with methanol as a mobile phase, with flow rate 1mL/min. Peaks were detected by UV absorption with a diode array detector. All final compounds were analyzed by LC/MS showing more than 96% purity. TLC analysis was carried out on aluminum sheets precoated with silica gel F_{254} (0.2 mm) from Aldrich.

7.2. General procedure for the synthesis of compounds 6–18 and 20–23

7.2.1. Methyl *trans*-3-(3-Chlorophenyl)propenoate (38e). Concentrated H_2SO_4 (0.1 mL) was added to a solution of *trans*-3-(3-chlorophenyl) propenoic acid (0.2 g,

1.09 mmol) in MeOH (5 mL). The solution was heated at reflux overnight. After cooling the solution, the acid was neutralized with saturated aqueous Na_2CO_3. The aqueous solution was extracted with ether (3 × 50 mL). The organic phase was washed with brine, dried over Na_2SO_4, filtered, and concentrated. The residue was purified by flash chromatography on silica gel (ether/petroleum ether 1:9), to give **38e** as a white solid. ^{1}H NMR ($CDCl_3$, 300,MHz) δ 7.63 (d, $J = 16.0$ Hz 1H), 7.51 (br s, 1H), 7.34–7.26 (m, 2H), 6.43 (d, $J = 16.0$ Hz 1H), 3.81 (s, 3H).

7.2.2. *trans*-2-(3-Chlorophenyl)-cyclopropanecarboxylic acid methyl ester (39e). Diazomethane was generated with a diazomethane-generating glassware kit (Aldrich). A solution of *N*-methyl-*N*-nitroso-4-toluenesulfonamide (Diazald, 2.23 g, 10.4 mmol) in ether (24 mL) was added dropwise to a mixture of KOH (1.75 g, 31.2 mmol) in H_2O (18 mL), ether (4 mL), and 2-(2-ethoxyethoxy)ethanol (18 mL) kept at 70 °C. The ethereal solution of diazomethane was continuously distilled into a stirred solution of **38a** (206 mg, 1.05 mmol) and $Pd(OAc)_2$ (1.16 mg, 0.00052) in CH_2Cl_2/ether (28/10 mL) kept at 0 °C. The rate of distillation was controlled to match the rate of addition. After the addition of Diazald was complete, the solution of **38a** was stirred at rt for 30 min. The excess of diazomethane was destroyed with acetic acid. The resulting mixture was washed with a saturated solution of $NaHCO_3$, brine, dried over Na_2SO_4, filtered, and concentrated. NMR confirmed the resulting product to be pure **39e**, to be used for the next reaction without further purification. ^{1}H NMR ($CDCl_3$, 300 MHz) δ 7.21–7.18 (m, 2H), 7.08–7.07 (m, 1H), 7.00–6.97 (m, 1H), 3.72 (s, 3H), 2.53–2.46 (m, 1H), 1.93–1.87 (m, 1H), 1.64–1.59 (m, 1H), 1.34–1.29 (m, 1H).

7.2.3. *trans*-2-(3-Chlorophenyl)-cyclopropanecarboxylic acid (40e). Aqueous NaOH (2 M, 3 mL) was added to a solution of **39e** (200 mg, 1.13 mmol) in MeOH (2 mL), and the mixture was stirred for 2 h at rt. The mixture was concentrated and H_2O (20 mL) was added. The aqueous phase was washed with ether, acidified with 3 M aqueous HCl, and extracted with ether (20 mL × 3). The combined organic phases were dried over Na_2SO_4, filtered, and concentrated to give pure **40e**. ^{1}H NMR ($CDCl_3$, 300 MHz) δ 7.23–7.20 (m, 2H), 7.10–7.08 (m, 1H), 7.02–6.98 (m, 1H), 2.61–2.54 (m, 1H), 1.93–1.89 (m, 1H), 1.71–1.65 (m, 1H), 1.44–1.37 (m, 1H).

7.2.4. *trans*-2-(3-Chlorophenyl)-cyclopropylamine (41e). A mixture of **40e** (105 mg, 0.72 mmol) in dry *t*-BuOH (1.3 mL), diphenylphosporazidate (170 μL, 0.8 mmol), and triethylamine (105 μL, 1 mmol) was stirred at 90 °C under nitrogen atmosphere for 48 h. The solution was concentrated and poured into 10% aqueous Na_2CO_3 (20 mL) and extracted with ether (10 mL × 3). The combined organic phases were dried over Na_2SO_4, filtered, and concentrated. The resulting *t*-butyl carbamate was dissolved in MeOH (3 mL), and 1 M aqueous HCl (5 mL) was added. The solution was maintained at reflux overnight. Then the mixture was cooled and concentrated. The solution was washed with ether (10 mL × 3), and the aqueous phase was alkalinized with 10% aqueous K_2CO_3 until pH 10. The mixture was extracted with EtOAc (10 mL × 3). The combined organic phases were dried over K_2CO_3, filtered, and concentrated. The residue was purified by PTLC (chloroform/methanol 9:1) to give **41e**. ^{1}H NMR ($CDCl_3$, 300 MHz) δ 7.19–7.08 (m, 2H), 6.98–6.96 (m, 1H), 6.91–6.88 (m, 1H), 2.56–2.52 (m, 1H), 1.86–1.81 (m, 1H), 1.80–1.48 (br s, 2H), 1.11–1.04 (m, 1H), 1.00–0.94 (m, 1H).

7.2.5. *trans*-2-(3-Chlorophenyl)-cyclopropyladenosine (10). Compound **41e** (12 mg, 0.07 mmol) and 6-chloropurine riboside (25.8 mg, 0.09) were placed in a sealed tube with absolute ethanol (1 mL) and triethylamine (10 μL) and heated at 80 °C for 8 h. The solution was evaporated and the residue dissolved in chloroform (10 mL) and washed with H_2O (10 mL × 3). The organic phase was dried over Na_2SO_4, filtered, and concentrated. The residue was purified by PTLC (chloroform/methanol 9:1) to give pure **10**. ^{1}H NMR ($CDCl_3$, 300 MHz) δ 8.23–8.21 (m, 1H), 7.77–7.76 (m, 1H), 7.22–7.08 (m, 4H), 6.48 (br s, 1H), 6.16 (br s, 1H), 5.79 (d, $J = 7.2$ Hz 1H), 5.05 (t, $J = 5.7$ Hz 1H), 4.46 (d, $J = 4.5$ Hz 1H), 4.34 (s, 1H), 3.94 (d, $J = 13.2$ Hz 1H), 3.78–3.75 (m, 1H), 3.18 (br s, 1H), 2.25–2.06 (m, 1H), 1.73–1.51 (m, 1H), 1.41–1.25 (m, 2H). HR-MS: calculated for $C_{19}H_{21}O_4N_5Cl$ 418.1282 found 418.1282.

7.2.6. N^6-[*trans*-2-(2-Methylphenyl)cyclopropyl]adenosine (6). Yield 45%. ^{1}H NMR ($CDCl_3$, 300 MHz) δ 8.18–8.15 (m, 1H), 7.76 (s, 1H), 7.18–7.14 (m, 4H), 6.72–6.65 (m, 1H), 6.36–6.31 (m, 1H), 5.79 (d, $J = 7.2$ Hz 1H), 5.02 (br s, 1H), 4.43 (d, $J = 4.5$ Hz 1H), 4.32 (s, 1H), 3.94 (d, $J = 13.2$ Hz 1H), 3.75–3.70 (m, 1H), 3.22 (br s, 1H), 2.40 (d, $J = 3$ Hz, 3H), 2.18–2.13 (m, 1H), 1.36–1.23 (m, 4H). MS (APCI) $m/z = 398$ (M+1).

7.2.7. N^6-[*trans*-2-(3-Methylphenyl)cyclopropyl]adenosine (7). Yield 49%. ^{1}H NMR ($CDCl_3$, 300 MHz) δ 8.19 (s, 1H), 7.74 (m, 1H), 7.22–7.15 (m, 1H), 7.05–6.95 (m, 3H), 6.29 (br s, 1H), 5.78–5.72 (m, 1H), 5.04 (m, 1H), 4.45 (m, 1H), 4.32 (s, 1H), 3.92 (d, $J = 13.2$ Hz 1H), 3.73 (d, $J = 13.2$ Hz 1H), 3.17 (s, 1H), 2.33 (s, 3H), 2.09 (m, 1H), 1.37–1.24 (m, 2H). MS (APCI) $m/z = 398$ (M+1).

7.2.8. N^6-[*trans*-2-(4-Methylphenyl)cyclopropyl]adenosine (8). Yield 47%. ^{1}H NMR ($CDCl_3$, 300 MHz) δ 8.32 (s, 1H), 7.78 (s, 1H), 7.11 (m, 2H), 6.17 (br s, 1H), 5.79 (d, $J = 7.8$ Hz 1H), 5.05 (m, 1H), 4.50 (d, $J = 3.8$ Hz 1H), 4.35 (s, 1H), 3.96 (d, $J = 13.2$ Hz 1H), 3.75 (d, $J = 13.2$ Hz 1H), 3.49 (s, 1H), 3.20 (m, 1H), 2.84 (br s, 1H), 2.33 (s, 3H), 2.16 (m, 1H), 1.29–1.25 (m, 2H). MS (APCI) $m/z = 398$ (M+1).

7.2.9. N^6-[*trans*-2-(2-Chlorophenyl)cyclopropyl]adenosine (9). Yield 40%. ^{1}H NMR ($CDCl_3$, 300 MHz) δ 8.17–8.16

(m, 1H) 7.76 (s, 1H), 7.78–7.77 (m, 1H), 7.38–7.35 (m, 1H), 7.21–7.11 (m, 4H), 6.72–6.65 (br m, 1H), 6.48–6.31 (br m, 1H), 5.79–5.78 (m, 1H), 5.01 (br s, 1H), 4.45 (br s, 1H), 4.32 (s, 1H), 3.94 (d, $J = 13.2$ Hz 1H), 3.75–3.70 (m, 1H), 3.52 (br s, 1H), 3.15(br s, 1H), 2.48 (m, 1H), 1.77 (br s, 1H), 1.43–1.23 (m, 4H). MS (APCI) $m/z = 418$ (M+1).

7.2.10. N^6-[*trans*-2-(4-Chlorophenyl)cyclopropyl]adenosine (11). Yield 42%. ^{1}H NMR ($CDCl_3$, 300 MHz) δ 8.35 (s, 1H), 7.80 (s, 1H), 7.32–7.15 (m, 4H), 6.27 (br m, 1H), 6.09 (br s, 1H), 5.80 (d, $J = 7.8$ Hz 1H), 5.06 (br s, 1H), 4.51 (d, $J = 3.8$ Hz 1H), 4.35 (s, 1H), 3.96 (d, $J = 13.2$ Hz 1H), 3.78–3.73 (m, 1H), 3.25 (br s, 1H), 2.74 (br s, 1H), 2.14 (m, 1H), 1.33–1.25 (m, 2H). MS (APCI) $m/z = 418$ (M+1).

7.2.11. N^6-[*trans*-2-(3-Fluorophenyl)cyclopropyl]adenosine (12). Yield 35%. ^{1}H NMR ($CDCl_3$, 300 MHz) δ 8.25 (s, 1H), 8.15 (s, 1H) 7.86–7.24 (m, 4H), 7.07 (br s, 1H), 7.02 (br s, 1H), 5.79 (d, $J = 7.8$ Hz 1H), 5.15 (m, 1H), 4.52–4.30 (m, 2H), 3.95–3.72 (m, 2H), 2.93–2.85 (m, 1H), 2.35 (br s, 1H), 1.43–1.20 (m, 2H). MS (APCI) $m/z = 402$ (M+1).

7.2.12. N^6-[*trans*-2-(3,5-Difluorophenyl)cyclopropyl]adenosine (13). Yield 40%. ^{1}H NMR ($CDCl_3$, 300 MHz) δ 8.35 (s, 1H) 7.81 (s, 1H), 6.78–6.66 (m, 3H), 6.09 (br s, 1H), 5.80 (d, $J = 7.8$ Hz 1H), 5.07 (br s, 1H), 4.50 (br s, 1H), 4.35 (s, 1H), 5.96 (d, $J = 12$ Hz, 1H), 3.76 (d, $J = 12$ Hz, 1H), 3.21 (br s, 1H), 2.77 (br s, 1H), 2.17 (m, 1H), 1.35–1.15 (m, 2H). MS (APCI) $m/z = 420$ (M+1).

7.2.13. N^6-[*trans*-2-(3-Trifuoromethyloxyphenyl)cyclopropyl]adenosine (14). Yield 30%. ^{1}H NMR ($CDCl_3$, 300 MHz) δ 8.35 (s, 1H), 8.18 (s, 1H) 7.96–7.34 (m, 4H), 7.07 (br s, 1H), 7.02 (br s, 1H), 5.79 (d, $J = 7.8$ Hz 1H), 5.05 (m, 1H), 4.51–4.34 (m, 2H), 3.97–3.70 (m, 2H), 2.92–2.85 (m, 1H), 2.32 (br s, 1H), 1.41–1.25 (m, 2H). MS (APCI) $m/z = 468$ (M+1).

7.2.14. N^6-[*trans*-2-(3-Nitrophenyl)cyclopropyl]adenosine (15). Yield 42%. ^{1}H NMR ($CDCl_3$, 300 MHz) δ 8.26–8.16 (m, 1H), 8.15 (br s, 1H), 8.07 (d, $J = 8.4$ Hz, 1H), 7.82 (s, 1H), 7.60–7.57 (m, 1H), 7.50–7.39 (m, 4H), 5.85 (d, $J = 6.3$ 1H), 5.02 (t, $J = 6.5$ Hz, 1H), 4.47 (br s, 1H), 4.35 (s, 1H), 3.97 (d, $J = 13.2$ Hz 1H), 3.78–3.73 (m, 1H), 3.17 (br s, 1H), 2.25 (m, 1H), 1.50–1.41 (m, 2H). MS (APCI) $m/z = 429$ (M+1).

7.2.15. N^6-[*trans*-2-(3-Aminophenyl)cyclopropyl]adenosine (18). Yield 35%. ^{1}H NMR (CD_3OD, 300 MHz) δ 8.26 (s, 2H), 7.02 (t, $J = 7.8$ Hz, 1H), 6.56 (t, $J = 7.8$ Hz, 3H), 5.96 (d, $J = 6.6$, 1H), 4.76–4.72 (m, 1H), 4.33–4.31 (m, 1H), 4.17–4.16 (m, 1H), 3.91–3.71 (m, 2H), 2.15–2.07 (m, 1H), 1.35–1.22 (m, 2H). MS (APCI) $m/z = 399$ (M+1).

7.2.16. N^6-[*trans*-2-(3-Acetamidophenyl)cyclopropyl]-adenosine (19). Yield 39%. ^{1}H NMR (CD_3OD, 300 MHz) δ 8.26 (br s, 2H), 7.43–7.36 (m, 2H), 7.25–7.19 (m, 1H), 6.97–6.95 (m, 1H), 5.97 (d, $J = 6.6$, 1H), 4.36–4.31 (m, 1H), 4.17–4.14 (m, 1H), 3.92–3.87 (m, 2H), 3.25–3.07 (m, 1H), 2.17–2.04 (m, 4H), 1.38–1.23 (m, 2H). MS (APCI) $m/z = 441$ (M+1).

7.2.17. N^6-[*trans*-2-(2-Cyanophenyl)cyclopropyl]adenosine (20). Yield 45%. ($CDCl_3$, 300 MHz) δ 8.27 (s, 1H) 7.83 (s, 1H), 7.33–7.30 (m, 1H), 7.29–7.20 (m, 3H), 6.19–6.03 (m, 2H), 5.79 (d, $J = 7.2$ Hz 1H), 5.05 (m, 1H), 4.48 (m, 1H), 4.34 (s, 1H), 3.94 (d, $J = 13.2$ Hz 1H), 3.81–3.75 (m, 1H), 3.22 (m, 1H), 2.95–2.86 (m, 1H), 2.12–2.08 (m, 1H), 1.48–1.25 (m, 2H). MS (APCI) $m/z = 408$ (M+1).

7.2.18. N^6-[*trans*-2-(3-Methoxyphenyl)cyclopropyl]adenosine (21). Yield 38%. ^{1}H NMR ($CDCl_3$, 300 MHz) δ 8.24 (s, 1H), 7.77 (br s, 1H), 6.85–6.72 (m, 3H), 6.25 (br s, 1H), 5.79 (br s, 1H), 5.05 (m, 1H), 4.48–4.34 (m, 2H), 3.96–3.72 (m, 6H), 3.20 (br s, 1H), 2.17 (m, 1H), 1.50–1.38 (m, 2H). MS (APCI) $m/z = 414$ (M+1).

7.2.19. N^6-[*trans*-2-(3-Trifluoromethylphenyl)cyclopropyl]adenosine (22). Yield 30%. ^{1}H NMR ($CDCl_3$, 300 MHz) δ 8.34 (s, 1H), 7.8 1 (br s, 1H), 7.52–7.40 (m, 4H), 6.30 (br s, 1H), 6.12 (br s, 1H), 5.81 (d, $J = 6.9$, 1H), 5.07 (m, 1H), 4.48 (m, 1H), 4.35 (s, 1H), 3.97 (m, 1H), 3.81–3.75 (m, 1H), 3.25 (br s, 1H), 2.25 (m, 1H), 1.51–1.38 (m, 2H). MS (APCI) $m/z = 452$ (M+1).

7.2.20. N^6-[*trans*-2-[3,5-Di(trifluoromethyl)phenyl]cyclopropyl]adenosine (23). Yield 32%. ^{1}H NMR ($CDCl_3$, 300 MHz) δ 8.37 (s, 1H), 8.21 (s, 1H) 7.86–7.34 (m, 3H), 7.07 (br s, 1H), 6.99 (br s, 1H), 5.79 (d, $J = 7.8$ Hz 1H), 5.07 (m, 1H), 4.51–4.34 (m, 2H), 3.97–3.70 (m, 2H), 2.92–2.89 (m, 1H), 2.32 (br s, 1H), 1.31–1.25 (m, 2H). MS (APCI) $m/z = 520$ (M+1).

7.2.21. N^6-(2,2-Diphenylcyclopropyl)adenosine (24). Yield 52%. ^{1}H NMR ($CDCl_3$, 300 MHz) δ 8.31–8.24 (m, 2H), 7.51–7.13 (m, 10H), 6.48 (br s, 1H), 5.89 (br s, 1H), 5.61 (d, $J = 7.2$ Hz 1H), 4.91–4.87 (m 1H), 4.34 (d, $J = 4.5$ Hz 1H), 4.24 (m, 1H), 3.90–3.83 (m, 2H), 3.70–3.63 (m, 1H), 1.78–1.45 (m, 2H). MS (APCI) $m/z = 460$ (M+1).

7.2.22. N^6-[2-(3-Thienyl)cyclopropyl]adenosine (25). Yield 45%. ^{1}H NMR ($CDCl_3$, 300 MHz) δ 8.32 (s, 1H), 7.80 (s, 1H) 7.02–7.01 (m, 2H), 6.13 (br s, 1H), 5.81 (d, $J = 7.5$ Hz 1H), 5.06 (m, 1H), 4.50 (d, $J = 4.5$ Hz 1H), 4.35 (s, 1H), 3.96 (d, $J = 12.8$ Hz, 1H), 3.76 (d, $J = 12.8$ Hz, 1H), 3.22–3.13 (m, 1H), 2.82 (br s, 1H), 2.22–1.18 (m.1H), 1.31–1.20 (m, 2H). MS (APCI) $m/z = 390$ (M+1).

7.2.23. N^6-(Cyclopropyl)adenosine (32). Yield 65%. ^{1}H NMR ($CDCl_3$, 300 MHz) δ 8.25 (s, 1H), 7.77 (s, 1H) 6.46 (d, $J = 11.4$ Hz, 1H), 6.03 (br s, 1H), 5.79 (d, $J = 7.5$ Hz 1H), 5.06 (m, 1H), 4.48 (d, $J = 4.5$ Hz 1H), 4.34 (s, 1H), 3.94 (d, $J = 10.8$ Hz, 1H), 3.12–2.93 (m, 2H), 0.93 (d, $J = 6.9$, 2H), 0.66 (s, 1H). MS (APCI) $m/z = 308$ (M+1).

7.2.24. N^6-[2,2-Di-(phenylethyl)cyclopropyl]adenosine (33). Yield 60%. ^{1}H NMR ($CDCl_3$, 300 MHz) δ 8.13 (s, 1H), 7.59 (s, 1H) 7.32–7.17 (m, 10H), 6.01 (br s, 1H), 5.68 (d, $J = 7.2$ Hz 1H), 4.92 (t, $J = 6.5$ Hz 1H), 4.36–4.26 (m, 4H), 4.09 (br s, 1H), 3.90–3.86 (d, $J = 12.9$ Hz 1H), 3.73–3.66 (m, 2H). MS (APCI) $m/z = 448$ (M+1).

7.2.25. *trans*-2-(3-Acetamidophenyl)-cyclopropylamine (44). Ethylchloroformate (0.035 mL, 0.35 mmol) was added to a solution of **42** (50 mg, 0.25 mmol) and triethylamine (0.04 mL, 0.3 mmol) in dry acetone at −10 °C. The solution was stirred at the same temperature for 2 h, and a solution of NaN_3 (25 mg, 0.38 mmol) in H_2O (0.5 mL) was added. The stirring was interrupted after 1 h, and additional H_2O (5 mL) was added. The solution was concentrated and extracted with EtOAc (20 mL × 3). The combined organic layers were dried over Na_2SO_4, filtered, and concentrated. The residue was dissolved in toluene (50 mL), and the solution was concentrated by half to eliminate traces of H_2O. The solution was heated at 90 °C for 2 h while observing N_2 evolution. Then the toluene was evaporated, and the resulting isocyanate was dissolved in dry 2-(trimethylsilyl)ethanol (2 mL) and the solution was heated to 60 °C overnight. The solution was cooled and concentrated. The residue was purified by flash chromatography on silica gel (ether/petroleum ether 1:9), to give the pure carbamate. The carbamate was treated with tetrabutylammonium fluoride (1 M solution in THF 0.28 mL, 0.28 mmol) at 50 °C for 24 h. The solution was cooled, and H_2O (5 mL) was added, and the resulting mixture was stirred for 20 min. Then it was concentrated, and the aqueous solution was acidified with 1 M HCl and washed with ether (20 mL × 3), and the aqueous phase was alkalinized with 10% aqueous Na_2CO_3. The mixture was extracted with EtOAc (10 mL × 3). The combined organic phases were dried over K_2CO_3, filtered, and concentrated. The residue was purified by PTLC (chloroform/methanol 9:1) to give **44**. ^{1}H NMR ($CDCl_3$, 300 MHz) δ 8.18–8.01 (m, 1H), 7.33–7.28 (m, 1H), 7.17–7.12 (m, 1H), 6.73–6.71 (m, 1H), 3.30–3.24 (m, 1H), 2.54 (br s, 1H), 2.18 (s, 3H), 1.87–1.83 (m, 1H), 1.61 (br s, 2H), 1.44–1.35 (m, 2H).

7.2.26. 2,2-Diphenylcyclopropanecarboxylic acid (47). 1,1-Diphenylethylene (1.02 g, 5.67 mmol), dry Cu_2SO_4 (58.3 mg, 0.36 mmol), and dry benzene (2 mL) were put in a three-necked flask equipped with two condensers and a dropping funnel. The solution was stirred and heated at 75 °C for 6 h. Ethyldiazoacetate (1.3 mL) was added dropwise over 1 h. The mixture was cooled to rt and stirred overnight. NaOH (1.45 g, 36 mmol) in ethanol (11.5 mL) was added, and the mixture was refluxed for 6 h. The solution was concentrated in vacuo, and H_2O (20 mL) was added. The aqueous mixture was heated to 90 °C and filtered and allowed to cool overnight. The crystals were filtered and redissolved in hot water, and the solution was filtered. The filtrate was acidified with 10% aqueous HCl, and the resulting precipitate was separated and identified as pure **47**. ^{1}H NMR ($CDCl_3$, 300 MHz) δ 7.38–7.35 (m, 2H), 7.27–7.12 (m, 8), 2.52–2.47 (m, 1H), 2.08–2.05 (m, 1H), 1.62–1.57 (m, 1H).

8. Pharmacology

8.1. Materials

[^{3}H]R-PIA and [^{125}I]I-AB-MECA were from Amersham Pharmacia Biotech (Piscataway, NJ), and [^{3}H]CGS21680 was from Perkin–Elmer. (Boston, MA). Adenosine deaminase was obtained from Sigma (St. Louis, MO). All other compounds were obtained from standard commercial sources and were of analytical grade.

8.2. Biological assays

The procedures for [^{3}H]R-PIA and [^{3}H]CGS21680 binding to A_1 and A_{2A} receptors, respectively, were as previously described.[7] Briefly, membranes (10–20 μg of protein) were incubated with radioligand and the competing adenosine derivative in duplicate, together with increasing concentrations of the competing compounds, in a final volume of 0.4 mL Tris·HCl buffer (50 mM, pH 7.4) at 25 °C for 60 min. Binding reactions were terminated by filtration through Whatman GF/B glass–fiber filters under reduced pressure with a MT-24 cell harvester (Gaithersburg, MD). Filters were washed three times with ice-cold buffer and placed in scintillation vials with 5 mL scintillation fluid, and bound radioactivity was determined by using a liquid scintillation counter. Functional assays of adenylyl cyclase (either stimulation via the hA_{2B} AR or inhibition via the hA_3AR) stably transfected CHO cells was carried out as previously described.[26]

8.3. Statistical analysis

Binding and functional parameters were estimated with GraphPAD Prism software (GraphPAD, San Diego, CA). IC_{50} values obtained from competition curves were converted to K_i values with the Cheng–Prusoff equation.[19] Data were expressed as mean ± standard error.

8.4. Molecular modeling

All calculations were performed on a Silicon Graphics Octane workstation (300 MHz, MIPS R12000 (IP30) processor, Mountain View, CA). All ligand structures

were constructed using the Sketch Molecule of SYBYL 6.9.[20] A conformational search of compounds **3** and **4** to be docked was performed by random search for all rotatable bonds. The options of random search were 3,000 iteration, 3 kcal energy cutoffs, and chirality checking. In all cases, MMFF force field[27] and charge were applied using distance-dependent dielectric constants and conjugate gradient method until the gradient reached to 0.05 kcal/mol/Å. After clustering the low-energy conformers from the result of the conformational search, the representative conformers from all groups were reoptimized by semiempirical molecular orbital calculations with the PM3 method in the MOPAC 6.0 package.[28]

A hA_3AR model (PDB code: 1o74) constructed by homology to the high-resolution X-ray structure of bovine rhodopsin[17] was used for the docking study. The (1*S*,2*R*)-isomers of all ligands in Table 1 were docked within the hA_3AR model. The atom types were manually assigned with the Amber all atom force field[29] and their charges were calculated before docking. The starting geometry of ligand conformation was chosen from the hA_3AR complex model with Cl-IB-MECA, which was already validated by point mutation.[6] The ribose-binding position of this series was fixed by an atom-by-atom fitting method for the carbon atoms of the ribose ring. Only N^6-binding regions were variously positioned in the putative binding cavity, rotating the flexible bonds of N^6 substituents, t_0 and t_1 angles. Several conformations without any steric bump were selected for further optimization. The initial structures of all complexes were optimized with the Amber force field with a fixed dielectric constant of 4.0 and terminating gradient of 0.1 kcal mol^{-1} $Å^{-1}$. Binding energy was calculated by the following equation: binding E=complex E−(receptor E+ligand E). These energies are not rigorous thermodynamic quantities but can only be used to compare the relative stabilities of the complexes. Consequently, these interaction energy values cannot be used to calculate binding affinities because changes in entropy and solvation effects are not taken into account. In addition, nonbonding van der Waals and electrostatic energies were calculated.

For the training set of 3D-QSAR, two models were generated. In model 1, a series of energetically favorable, bound conformations from the docking complex were selected and aligned in the 3D Cartesian space, and similar conformations for the t_0, t_1, and t_2 binding preference were used for model 2. The K_i values of hA_3AR for the training set were converted to pK_i ($-\log K_i$) values as dependent variables in the CoMFA and CoMSIA. To derive the CoMFA and CoMSIA descriptors as independent variables, a 3D cubic lattice was automatically generated as a single grid with 2 Å space, overlapping all aligned molecules and extended by at least 4 Å along all axes. The steric fields were calculated with a Lennard–Jones potential and the electrostatic fields were calculated with a Coulombic potential at each lattice of a sp^3 carbon probe atom with a van der Waals radius of 1.52 Å and a charge of +1.0. The default energy cutoff of 30 kcal/mol was used.

CoMSIA descriptors were derived from the same lattice box used for the CoMFA calculations. For the calculation of CoMSIA similarity indices, five different similarity fields including steric, electrostatic, hydrophobic, H-bond donor, and H-bond acceptor were calculated at the regularly spaced grid points with a common probe atom with radius of 1 Å, charge, hydrophobicity, and H-bonding properties of +1. A Gaussian function with the default value (0.3) of the attenuation factor, α, was used for the distance dependence between the molecule and the probe atoms. The steric CoMSIA fields were from the internally coded parameters of the van der Waals table in SYBYL program. The electrostatic fields were calculated from the atomic partial charge of MMFF94. The hydrophobic fields were derived from atom-based values based on the research of Viswanadhan et al.[38] The H-bond donor and acceptor fields were obtained by a rule-based method from experimental values, creating dummy atoms at donor and acceptor sites like extension points of DISCO (distance comparisons).[37]

The PLS regression analyses[39] were used to derive a linear relationship. The predictive value of the models was evaluated first by SAMPLS (sample distance partial least squares)[40] and then by leave-one-out cross-validation, with a 2 kcal/mol column filtering with a column scaling of CoMFA standard. The outlier points whose target values were badly predicted in the residual plot from the cross-validation analyses were omitted to get the predictable model with a sufficiently high q^2 value (>0.4). For the conventional r^2 value, final noncross-validation with the number of components to the optimum value from the cross-validation analysis was performed. CoMFA and CoMSIA stdev * coeff contour maps were generated by a default value of contribution.

Acknowledgements

Dr. Neli Melman thanks the Cystic Fibrosis Foundation for financial support. We thank Dr. Tom Spande and Dr. Victor Livengood (NIDDK) for mass spectral measurements.

References and notes

1. Fredholm, B. B.; IJzerman, A. P.; Jacobson, K. A.; Klotz, K.-N.; Linden, J. *Pharm. Rev.* **2001**, *53*, 527.
2. von Lubitz, D. K. J. E.; Lin, R. C.-S.; Popik, P.; Carter, M. F.; Jacobson, K. A. *Eur. J. Pharmacol.* **1994**, *263*, 59.
3. Ohta, A.; Sitkovsky, M. *Nature* **2001**, *414*, 916.
4. Stambaugh, K.; Jacobson, K. A.; Jiang, J.-l.; Liang, B. T. *Am. J. Physiol.* **1997**, *273*, H501–H505.
5. Fishman, P.; Madi, L.; Bar-Yehuda, S.; Barer, F.; Del Valle, L.; Khalili, K. *Oncogene* **2002**, *21*, 4060.
6. Gao, Z.-G.; Kim, S.-K.; Biadatti, T.; Chen, W.; Lee, K.; Barak, D.; Kim, S. G.; Johnson, C. R.; Jacobson, K. A. *J. Med. Chem.* **2002**, *45*, 4471.
7. Gao, Z.-G.; Blaustein, J.; Gross, A. S.; Melman, N.; Jacobson, K. A. *Biochem. Pharmacol.* **2003**, *65*, 1675.

8. Kim, S.-K.; Gao, Z.-G.; Van Rompaey, P.; Gross, A. S.; Chen, A.; Van Calenbergh, S.; Jacobson, K. A. *J. Med. Chem.* **2003**, *46*, 4847.
9. Gao, Z-G.; Jeong, L. S.; Moon, H. R.; Kim, H. O.; Choi, W. J.; Shin, D. H.; Elhalem, E.; Comin, M. J.; Melman, N.; Mamedova, L.; Gross, A. S.; Rodriguez, J. B.; Jacobson, K. A. *Biochem. Pharmacol.* **2004**, *67*, 893–901.
10. Zablocki, J.A.; Wu, L.; Shryock, J.; Belardinelli, L. *Curr. Top. Med. Chem.* **2003**, in press.
11. Williams, M.; Risley, E. A. *Proc. Nat. Acad. Sci. USA* **1980**, *77*, 6892.
12. Vallgårda, J.; Appelberg, U.; Arvidsson, L.-E.; Hjorth, S.; Svensson, B. E.; Hacksell, U. *J. Med. Chem.* **1996**, *39*, 1485.
13. Trivedi, B. K.; Blankley, C. J.; Bristol, J. A.; Hamilton, H. W.; Patt, W. C.; Kramer, W. J.; Johnson, S. A.; Bruns, R. F.; Cohen, D. M.; Ryan, M. J. *J. Med. Chem.* **1991**, *34*, 1043.
14. Daly, J. W.; Padgett, W.; Thompson, R. D.; Kusachi, S.; Bungi, W. J.; Olsson, R. A. *Biochem. Pharmacol.* **1986**, *35*, 2467.
15. Knutsen, L. J.; Lau, J.; Petersen, H.; Thomsen, C.; Weis, J. U.; Shalmi, M.; Judge, M. E.; Hansen, A. J.; Sheardown, M. J. *J. Med. Chem.* **1999**, *42*, 3463.
16. Gallo-Rodriguez, C.; Ji, X.-D.; Melman, N.; Siegman, B. D.; Sanders, L. H.; Orlina, J.; Fischer, B.; Pu, Q.-L.; Olah, M. E.; van Galen, P. J. M.; Stiles, G. L.; Jacobson, K. A. *J. Med. Chem.* **1994**, *37*, 636.
17. Palczewski, K.; Kumasaka, T.; Hori, T.; Behnke, C. A.; Motoshima, H.; Fox, B. A.; Le Trong, I.; Teller, D. C.; Okada, T.; Stenkamp, T. E.; Yamamoto, M.; Miyano, M. *Science* **2000**, *289*, 739.
18. Fossetta, J.; Jackson, J.; Deno, G.; Fan, X.; Du, X. K.; Bober, L.; Soude-Bermejo, A.; de Bouteiller, O.; Caux, C.; Lunn, C.; Lundell, D.; Palmer, R. K. *Mol. Pharmacol.* **2003**, *63*, 342.
19. Cheng, Y.-C.; Prusoff, W. H. *Biochem. Pharmacol.* **1973**, *22*, 3099.
20. Sybyl Molecular Modeling System, version 6.9; Tripos Inc., St. Louis, Missouri 63144, USA.
21. Blatchford, J. K.; Orchin, M. *J. Org. Chem.* **1964**, *29*, 839.
22. Parsons, M.; Young, L.; Lee, J.-E.; Jacobson, K. A.; Liang, B. T. *FASEB J.* **2000**, *14*, 1423.
23. van Galen, P. J. M.; van Bergen, A. H.; Gallo-Rodriguez, C.; Melman, N.; Olah, M. E.; IJzerman, A. P.; Stiles, G. L.; Jacobson, K. A. *Mol. Pharmacol.* **1994**, *45*, 1101.
24. Jacobson, K. A.; Kim, H. S.; Ravi, G.; Kim, S. K.; Lee, K.; Chen, A.; Chen, W.; Kim, S. G.; Barak, D.; Liang, B. T.; Gao, Z.-G. *Drug Devel. Res.* **2003**, *58*, 330.
25. Klotz, K. N.; Hessling, J.; Hegler, J.; Owman, C.; Kull, B.; Fredholm, B. B.; Lohse, M. J. *Naunyn Schmiedeberg's Arch. Pharmacol.* **1998**, *357*, 1.
26. Nordstedt, C.; Fredholm, B. B. *Anal. Biochem.* **1990**, *189*, 231.
27. Halgren, T. A. *J. Comput. Chem.* **1999**, *20*, 730.
28. Stewart, J. J. P. *J. Comput. Aided Mol. Des.* **1990**, *4*, 1.
29. Cornell, W. D.; Cieplak, P.; Bayly, C. I.; Gould, I. R.; Merz, K. M., Jr; Ferguson, D. M.; Spellmeyer, D. C.; Fox, T.; Caldwell, J. W.; Kollman, P. A. *J. Am. Chem. Soc.* **1995**, *117*, 5179.
30. Gao, Z.-G.; Kim, S.-K.; Gross, A. S.; Chen, A.; Blaustein, J. B.; Jacobson, K. A. *Mol. Pharmacol.* **2003**, *63*, 1021.
31. Jacobson, K. A.; Gao, Z.-G.; Chen, A.; Barak, D.; Kim, S.-A.; Lee, K.; Link, A.; Van Rompaey, P. V.; Van Calenbergh, S.; Liang, B. T. *J. Med. Chem.* **2001**, *44*, 4125.
32. The relative energy of the complex in the docking model of both of **16** and **17** depending on the three t_1 angles, −60°, 180°, and 60°, at the starting geometry was high, at least 15–30 kcal/mol, whereas the energy of the complex with **3** for three different t_1 angles was within 3 kcal/mol.
33. A series of various energetically favorable bound conformations for model 1 and similar bound conformations for model 2 were aligned in 3D-Cartesian space without RMS fitting of all molecules, because the alignment result obtained using RMS fitting of the ribose ring was not in close agreement with the 3D-QSAR.
34. Cramer, R. D., III; Patterson, D. E.; Bunce, J. D. *J. Am. Chem. Soc.* **1988**, *110*, 5959.
35. Cramer, R. D., III; DePriest, S. A.; Patterson, D. E.; Hecht, P. In *3D QSAR in Drug Design: Theory, Methods and Applications: The Developing Practice of Comparative Molecular Field Analysis*; Kubinyi, H., Ed.; ESCOM: Leiden, The Netherlands, 1993; p 443.
36. Klebe, G.; Abraham, U.; Mietzner, T. *J. Med. Chem.* **1994**, *37*, 4130.
37. Klebe, G.; Abraham, U. *J. Comput. Aided Mol. Des.* **1999**, *13*, 1.
38. Viswanadhan, V. N.; Ghose, A. K.; Revankar, G. R.; Robins, R. K. *J. Chem. Inf. Comput. Sci.* **1989**, *29*, 163.
39. Wold, S.; Albano, C.; Dunn, W. J., III; Edlund, U.; Esbensen, K.; Geladi, P.; Hellberg, S.; Johansson, E.; Lindberg, W.; Sjostrom, M. In *Chemometrics: Mathematics and Statistics in Chemistry: Multivatiate Data Analysis in Chemistry*; Wold Kowalski, B., Ed.; Reidel: Dordrecht, Netherlands, 1984; p 17.
40. Bush, B. L.; Nachbar, R. B., Jr. *J. Comput. Aided Mol. Des.* **1993**, *7*, 587.